



Enterohaemorrhagic *E. coli* modulates an ARF6:Rab35 signaling axis to prevent recycling endosome maturation during infection

R. Christopher D. Furniss, Sabrina Slater, Gad Frankel and Abigail Clements

MRC Centre for Molecular Bacteriology and Infection, Department of Life Sciences, Imperial College London, London, SW7 2AZ

Correspondence to Abigail Clements: a.clements@imperial.ac.uk

<http://dx.doi.org/10.1016/j.jmb.2016.05.023>

Edited by Charalampo Kalodimos

Abstract

Enteropathogenic and enterohaemorrhagic *Escherichia coli* (EPEC/EHEC) manipulate a plethora of host cell processes to establish infection of the gut mucosa. This manipulation is achieved via the injection of bacterial effector proteins into host cells using a Type III secretion system. We have previously reported that the conserved EHEC and EPEC effector EspG disrupts recycling endosome function, reducing cell surface levels of host receptors through accumulation of recycling cargo within the host cell. Here we report that EspG interacts specifically with the small GTPases ARF6 and Rab35 during infection. These interactions target EspG to endosomes and prevent Rab35-mediated recycling of cargo to the host cell surface. Furthermore, we show that EspG has no effect on Rab35-mediated uncoating of newly formed endosomes, and instead leads to the formation of enlarged EspG/TfR/Rab11 positive, EEA1/Clathrin negative stalled recycling structures. Thus, this paper provides a molecular framework to explain how EspG disrupts recycling whilst also reporting the first known simultaneous targeting of ARF6 and Rab35 by a bacterial pathogen.

© 2016 The Authors. Published by Elsevier Ltd. This is an open access article under the CC BY license (<http://creativecommons.org/licenses/by/4.0/>).

Introduction

The attaching and effacing (A/E) pathogens enterohaemorrhagic *Escherichia coli* (EHEC) and enteropathogenic *E. coli* (EPEC) use a type III secretion system (T3SS) to deliver an array of bacterial effector proteins into host cells during infection, facilitating colonization of the gut epithelia [1]. EHEC regularly causes food-poisoning outbreaks, with associated diarrhea, hemorrhagic colitis and hemolytic uremic syndrome, and remains the leading cause of acute pediatric renal failure in the UK and US [2,3]. EPEC causes illness in young children in low-income countries and is responsible for significant morbidity and mortality due to diarrheal disease.

Recently we demonstrated that EHEC depletes a number of cell surface receptors from the Plasma Membrane (PM) during infection, in a manner dependent on the T3SS effector EspG [4]. Amongst the cell surface receptors depleted is the Transferrin Receptor (TfR), the prototypical recycling protein, which cycles between the PM and the early and recycling endosome compartments [5]. We demonstrated that the

reduction in TfR levels on the cell surface is not due to degradation, as total cellular levels of TfR are unaltered during infection, and that injection of EspG results in the movement of the TfR to cytosolic vesicles positive for markers of recycling endosomes [4,6,7]. Therefore, we hypothesize that EspG may inhibit the recycling of internalized cell surface receptors back to the PM. Glotfelty et al. (2014) [8] recently described a similar observation, reporting the accumulation of internalized occludin within EPEC infected cells and an EspG1/G2-dependent accumulation of other tight junction proteins within the cytosol. Gill et al. (2007) [9] described the EspG-dependent movement of the major apical anion exchanger DRA away from the PM to intracellular compartments during EPEC infection and showed that EspG-mediated reduction of DRA at the plasma membrane is due to a decrease in DRA exocytosis [10]. These observations support our hypothesis that EspG influences the protein composition of the host plasma membrane through modulation of recycling endosomes.

Since its discovery in 2001 [11] the role of EspG has been extensively studied [9,12–19], although

its function during infection has remained controversial. EspG is now understood to modulate host endomembrane trafficking by functioning as a “catalytic scaffold” [20]. EspG has been shown to bind active, GTP-bound, ARF GTPases and to act as a Rab GTPase activating protein (GAP) [21]. Co-crystallization experiments [21] suggest EspG can bind ARF6 and Rab1 on its opposing surfaces, in a similar manner to the interactions originally described between EspG, ARF1 and p21-activated kinase (PAK) [20], raising the possibility that EspG may reorganize multiple host signaling networks during infection.

Our investigation of the small GTPase interacting partners of EspG during infection reveals that EspG modulates an ARF6:Rab35 signaling axis to disrupt recycling endosome function, resulting in the accumulation of recycling cargo within the host cytosol. Our results highlight the importance of spatial restriction of bacterial effector proteins during infection, whilst simultaneously providing a molecular mechanism to support previously published EspG phenotypes.

EspG interacts with ARF6 during infection

Humans express multiple ARF [5] and Rab (60+) proteins, each involved in specific membrane trafficking events (e.g. endoplasmic reticulum to Golgi, or early to late endosome). *In vitro* data indicates EspG can interact with at least 3 of the 5 ARF proteins (ARF 1, 5 and 6) [20]. However, the specificity of EspG interactions during infection remains unclear. To determine which ARF GTPases are genuine EspG interacting partners during infection we performed co-immunoprecipitation experiments using HeLa cells expressing a panel of GFP-tagged ARF GTPases infected with EHEC $\Delta espG + pEspG:4xHA$ (Fig. 1, replicate blots shown in Fig. S1). This revealed that EspG interacts primarily with ARF6 (Fig. 1a). ARF6 was also found to be the primary interacting partner over an infection time-course from 2.5 to 7.5 h of infection (data not shown), suggesting the ARF6 interaction occurs early during infection and is maintained as infection progresses.

Our previous observations regarding the localization of EspG during infection suggest EspG is not trafficking to the Golgi, as seen during ectopic expression [18,21] but is instead localized in endosomal compartments, with markers of recycling endosomes [4]. ARF 1,3, 4 and 5 have previously been described to localize predominantly to the Golgi [22] while ARF6 is mainly found at the plasma membrane and at endosomal sites [23]. These localizations were confirmed for the GFP-ARF fusions used in this work (Fig. S2). We observed that during EHEC infection ARF6 and EspG accumulated on the same endosomal structures. Calculation of Pearson's Correlation Coefficients for cells transfected with GFP-ARF6 and infected

with EHEC $\Delta espG + pEspG:4xHA$ indicates specific co-localization between ARF6 and EspG (Fig. 1b) consistent with the co-immunoprecipitation data (Fig. 1a).

EspG preferentially interacts with active ARF6 to localize at endosomal structures during infection

To determine if EspG interacts preferentially with GTP-bound ARF6 during infection we assessed the co-immunoprecipitation of EspG by constitutively inactive, GDP-bound (T44N) or constitutively active, GTP-bound (Q67L) ARF6 mutants [24]. Consistent with previous *in vitro* data [25], EspG was preferentially co-immunoprecipitated with GTP-bound rather than GDP-bound ARF6 (Fig. 2a).

ARF-binding has been proposed to spatially restrict EspG within host cells to allowing targeted, local Rab inactivation [21,25]. We therefore reasoned that ARF6 binding occurs upstream of interaction with Rabs and should therefore be independent of EspG's ability to act as a Rab GAP. Consistent with this hypothesis, an EspG Rab GAP mutant (EspG RQ) was co-immunoprecipitated by ARF6 during EHEC infection as efficiently as WT EspG (Fig. 2b). This hypothesis was further confirmed by the observation that cells expressing GDP-locked GFP-ARF6 T44N fail to show the characteristic endosomal localization of EspG, in contrast to un-transfected cells or those expressing WT GFP-ARF6 (Fig. 2c). Therefore the interaction of EspG with GTP-ARF6 is required for correct localization of EspG and is independent of EspG's Rab GAP activity.

EspG interacts with Rab35 during infection

Over 60 human Rab isoforms have been described to date [26]. We screened a panel of Rabs that have been described to localize at recycling endosomes or the trans-Golgi network [27]. This panel consisted of Rabs 8, 10, 11, 13, 22a, 30, 35, 37, 38 and 43a (Fig. S3). *In vitro* EspG was shown to act as a Rab GAP for only 12 of the 30 Rabs tested, including, in our panel, Rab 13, 30, 35, 37 and 38 [21]. We also included Rab1 in our panel as, *in vitro*, EspG showed the highest GAP activity for this protein [21].

Co-immunoprecipitation experiments using our Rab GTPase panel show that EspG is selectively and consistently immunoprecipitated by Rab35 (Fig. 3a, replicate blots shown in Fig. S4). EspG was also intermittently immunoprecipitated by Rab13, and then in decreasing amounts by Rabs 43a, 37 and 10. However Rab35 was the only Rab to immunoprecipitate EspG in every experiment. EspG was not co-immunoprecipitated by Rab1 in any experiment,

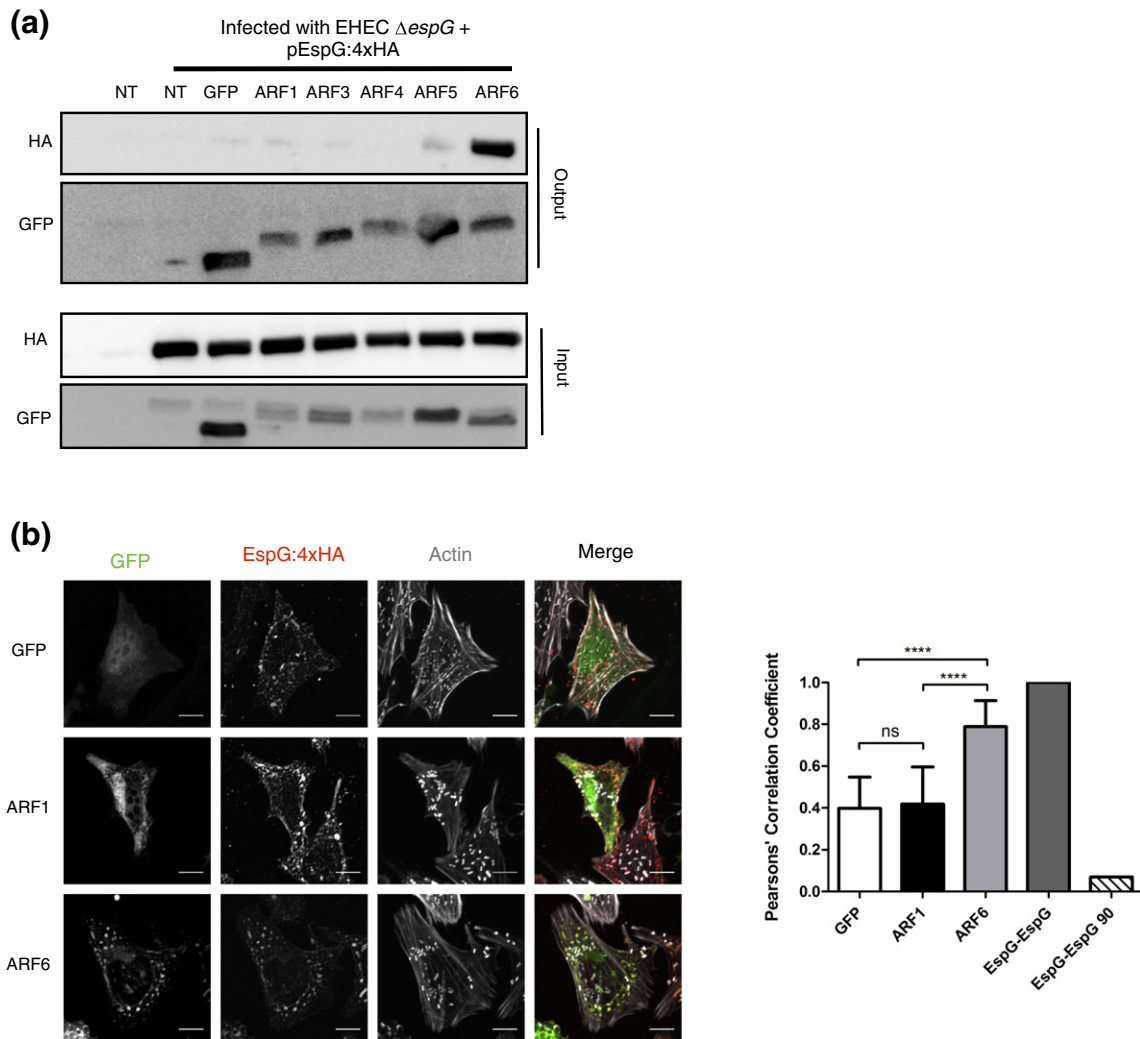


Fig. 1. EspG interacts with ARF6 during infection. a) HeLa cells expressing GFP-ARF fusions were infected with EHEC $\Delta espG$ + pEspG:4xHA. After 5 h of infection ARFs were immunoprecipitated (output, GFP) and co-immunoprecipitated EspG:4xHA detected (output, HA) ($n = 4$, see Fig. S1 for additional blots) b) Confocal microscopy suggests that GFP-ARF6 and EspG:4xHA colocalize on the same endosomal structures. Representative images show maximum intensity Z-projections, scale bars represent 5 μ m. Colocalization was quantified using Pearson's Correlation Coefficients generated for 20 fields of view (1–2 cells per image) across 2 independent experiments, graph shows means \pm SD, ns = non-significant, **** = $p < 0.0001$.

suggesting it is spatially removed from EspG during infection. Interestingly, Rab1 and Rab35 share significant sequence similarity at the amino acid level, and cluster in a distinct subfamily of Rab GTPases [28]. Therefore, whilst EspG is able to interact with and induce GTP hydrolysis of both Rab1 and Rab35 *in vitro*, spatial restriction of EspG to endosomal compartments during infection appears to direct EspG's GAP activity towards Rab35.

Co-localization analysis of EspG and GFP-Rab constructs shows that EspG co-localizes with Rab35, supporting our co-immunoprecipitation data (Fig. 3b). EspG also co-localizes with Rab11, a known marker of recycling endosomes. However, co-immuno-

precipitation of EspG by Rab11 was found to be no higher than with GFP alone, consistent with the absence of Rab GAP activity towards Rab11 *in vitro* [21]. These results indicate EspG localizes to ARF6/Rab35/Rab11 positive recycling endosomes during infection.

We propose that whilst EspG is capable of interacting with multiple ARF and Rab GTPases *in vitro*, during infection the spatial restriction of EspG limits its interacting partners. As such, it is the interactions with ARF6 (Fig. 1a) and Rab35 (Fig. 3a) that are relevant for EspG's function during infection. Our data suggests that during infection EspG is recruited to ARF6/Rab35 positive endosomal structures (Figs. 1c

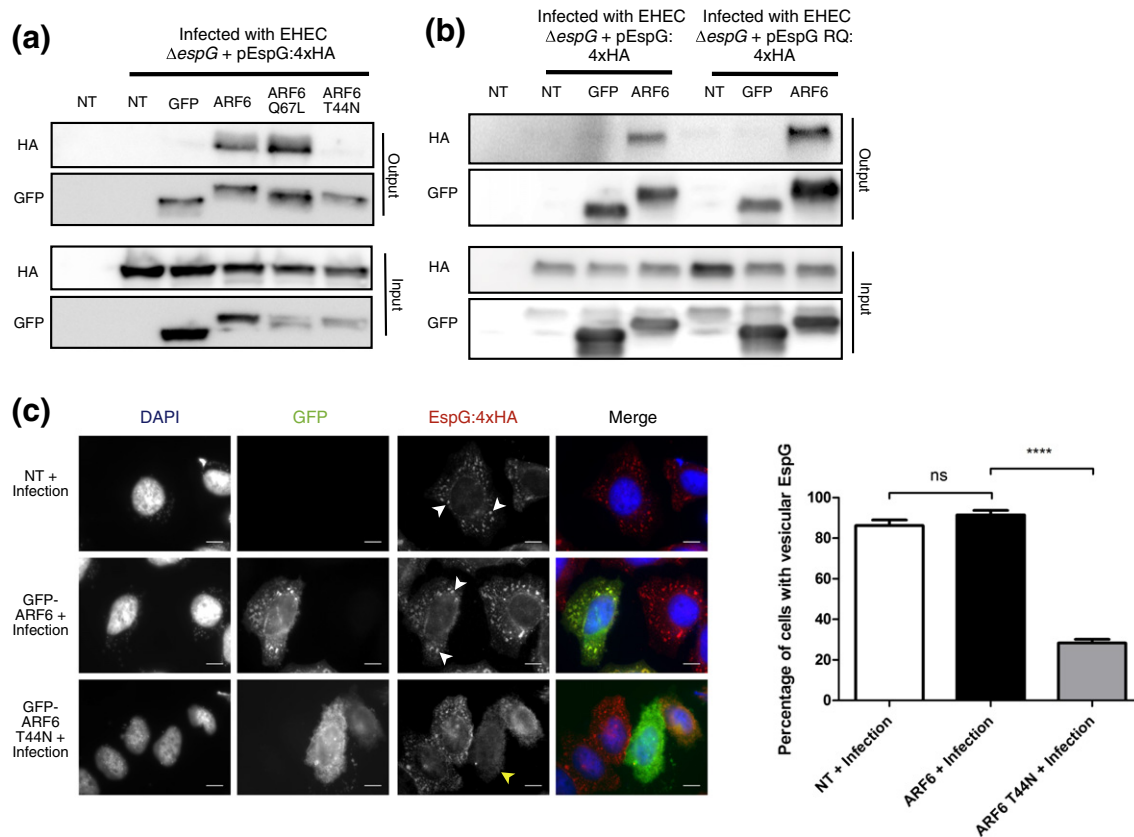


Fig. 2. EspG preferentially interacts with GTP-ARF6 upstream of Rab binding to target itself to endosomal structures. a) HeLa cells expressing GFP-ARF6 Q67L (GTP-locked) and T44N (GDP-locked) were infected with EHEC $\Delta espG + pEspG:4xHA$. After 5 h of infection ARFs were immunoprecipitated (output, GFP) and co-immunoprecipitated EspG:4xHA detected (output, HA) ($n = 4$) b) HeLa cells expressing GFP-ARF6 were then infected with EHEC $\Delta espG + pEspG:4xHA$ or EHEC $\Delta espG + pEspG RQ:4xHA$, GFP-ARF6 immunoprecipitated and co-immunoprecipitated EspG:4xHA or EspG RQ:4xHA detected ($n = 2$). c) HeLa cells expressing GFP-ARF6 or GFP-ARF6 T44N were infected with EHEC $\Delta espG + pEspG:4xHA$ for 5 h before the percentage of transfected cells exhibiting endosomal EspG:4xHA staining was scored. White arrowheads indicate EspG positive endosomal structures; yellow arrowheads indicate diffuse cytosolic EspG staining in cells expressing GFP-ARF6 T44N. Scale bars represent 10 μm . Graph shows means \pm SD of three independent experiments (> 100 cells counted per experiment) ns = non-significant, **** = $p < 0.0001$.

and 3c) through scaffolding with GTP-bound ARF6 (Figs. 1a and 2a). Targeting of EspG to these endosomal structures, via ARF6 (Fig. 2c), is necessary to ensure Rab hydrolysis only occurs for a specific Rab population, as previously postulated by Selyunin *et al.* [25]. During infection, this results in the Rab GAP activity of EspG being directed towards Rab35 (Fig. 3a).

Selyunin *et al.* also observed that binding of EspG to ARF-GTP may prevent access by ARF GAPs, thus locking the EspG-bound ARF in the GTP bound state. In this conformation the effector-binding surface of the ARF is unobstructed [25] raising the possibility that EspG, aside from using ARF-binding as a method of spatial restriction, also promotes the recruitment of ARF6 effectors. Importantly, as Rab GAP deficient EspG is able to interact with ARF6 (Fig. 2b), but unable to disrupt recycling [4], the functional disruption

of REs during infection appears to be dependent on EspG's Rab GAP activity. This does not preclude the stabilization of active ARF6 by EspG from playing another, currently unknown, role during infection.

Modulation of Rab35 by EspG does not influence vesicle uncoating after Clathrin-dependent endocytosis

Rab35 has been implicated in both endocytosis [29] and recycling of cargo [30,31,32]. We have previously demonstrated that EspG is able to disrupt cargo recycling [4] and were interested in whether EspG could also affect other Rab35 dependent activities. A recent report indicates that Rab35 has a role in the recruitment of Oculocerebrorenal Syndrome of Lowe (OCRL), an Inositol Polyphosphate 5-Phosphatase,

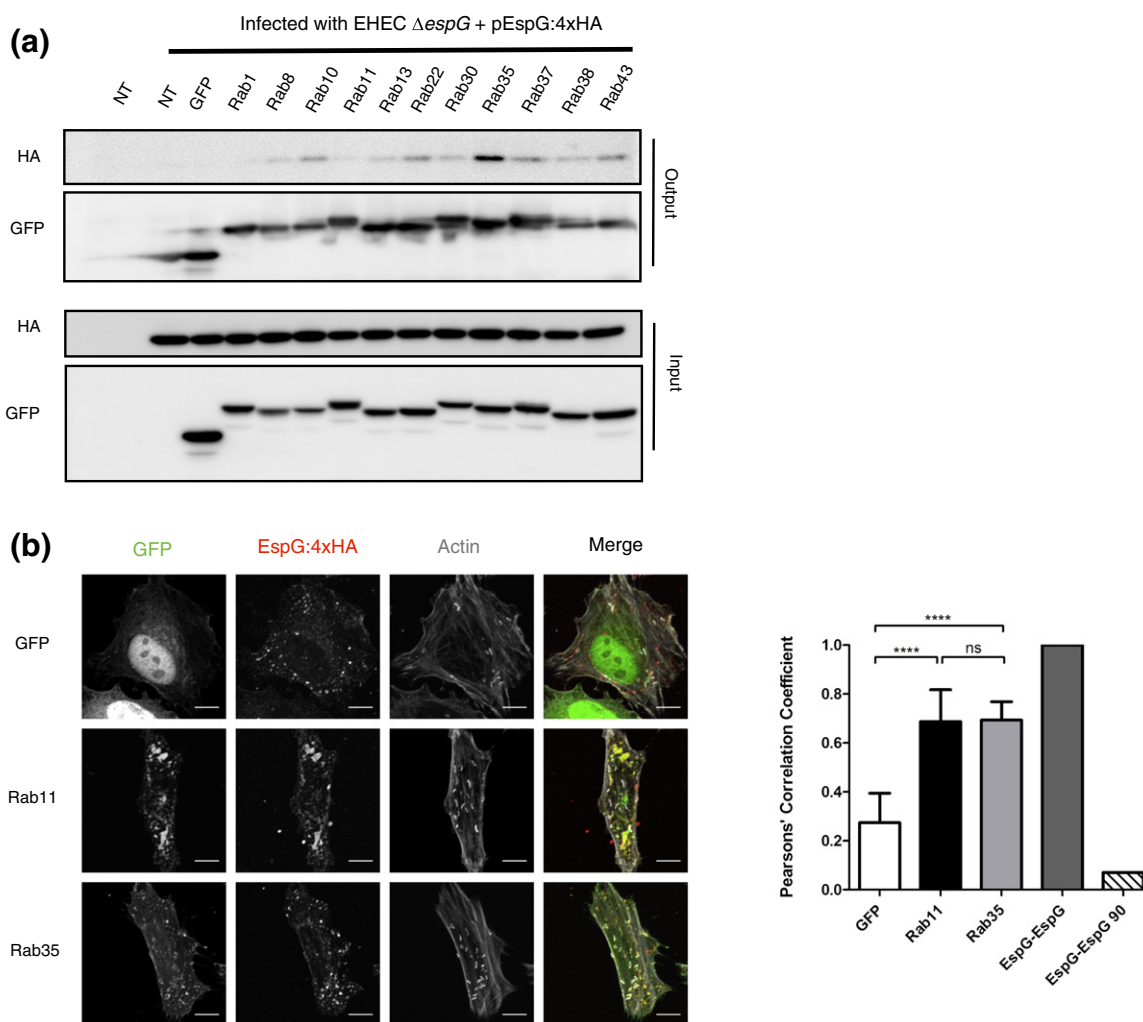


Fig. 3. EspG interacts and colocalizes with Rab35 during infection a) HeLa cells expressing GFP-Rab fusions were infected with EHEC $\Delta espG$ + pEspG:4xHA. After 5 h of infection Rabs were immunoprecipitated (output, GFP) and co-immunoprecipitated EspG:4xHA detected (output, HA) ($n = 5$ for all Rabs except Rab8 where $n = 2$, see Fig. S4 for additional blots) b) Confocal microscopy suggests that both GFP-Rab11 and GFP-Rab35 colocalize with EspG:4xHA on the same endosomal structures. Representative images show maximum intensity Z-projections, scale bars represent 5 μ m. Colocalization was quantified using Pearson's Correlation Coefficients generated for 20 fields of view (1–2 cells per image) across 2 independent experiments, graph shows means \pm SD, ns = non-significant, **** = $p < 0.0001$.

to newly formed endosomes. Recruitment of OCRL promotes the uncoating of Clathrin-Coated Vesicles (CCVs) after endocytosis [29]. To assess the effect of EspG on clathrin-uncoating of vesicles, HeLa cells expressing mRFP-clathrin light chain (CLC) were infected with WT EHEC, EHEC $\Delta espG$ and EHEC $\Delta espG$ + pEspG:4xHA and stained for TfR and Early Endosome Antigen 1 (EEA1). Peripheral endosomes containing TfR and EEA1 showed similar association with CLC in all conditions (Fig. 4a and b), unlike in Rab35 and OCRL siRNA treated cells [29]. However large TfR positive structures could be observed in WT EHEC, and to a greater extent in EHEC $\Delta espG$ + pEspG:4xHA infected cells, but not in uninfected cells or cells infected with EHEC $\Delta espG$.

These large TfR positive structures were negative for both EEA1 and CLC (Fig. 4b), and resemble the enlarged EspG/TfR positive vesicular structures seen previously [4]. These data suggest that EspG specifically targets Rab35 involved in recycling and not in recruitment of OCRL and CCV uncoating after endocytosis.

Whilst Rab35 has been implicated in early endocytic processes [29,33] ARF6 and Rab35 are also known to act antagonistically to control RE function, with ARF6 promoting the internalization of cell surface proteins and Rab35 mediating their recycling [30] via the assembly of a RE-bound signaling complex [32]. This Rab35-controlled complex also influences RE lipid composition [34] and vesiculation [31,35]. EspG

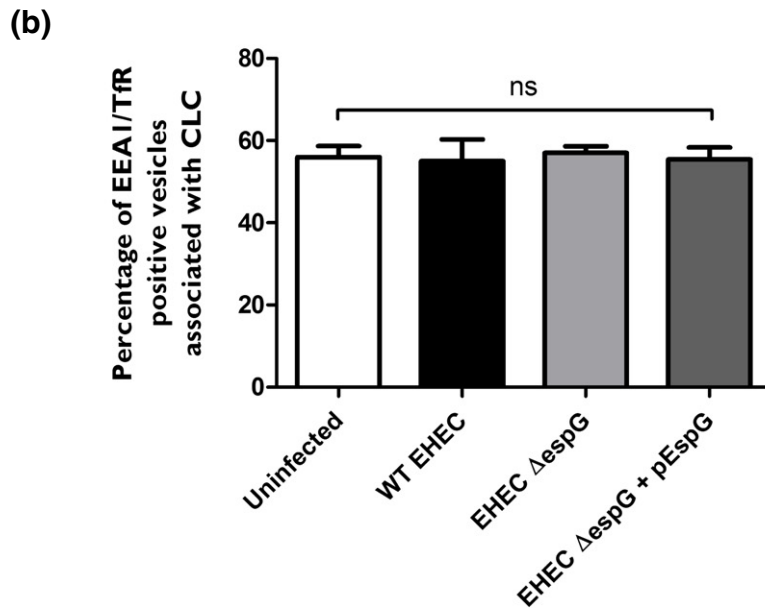
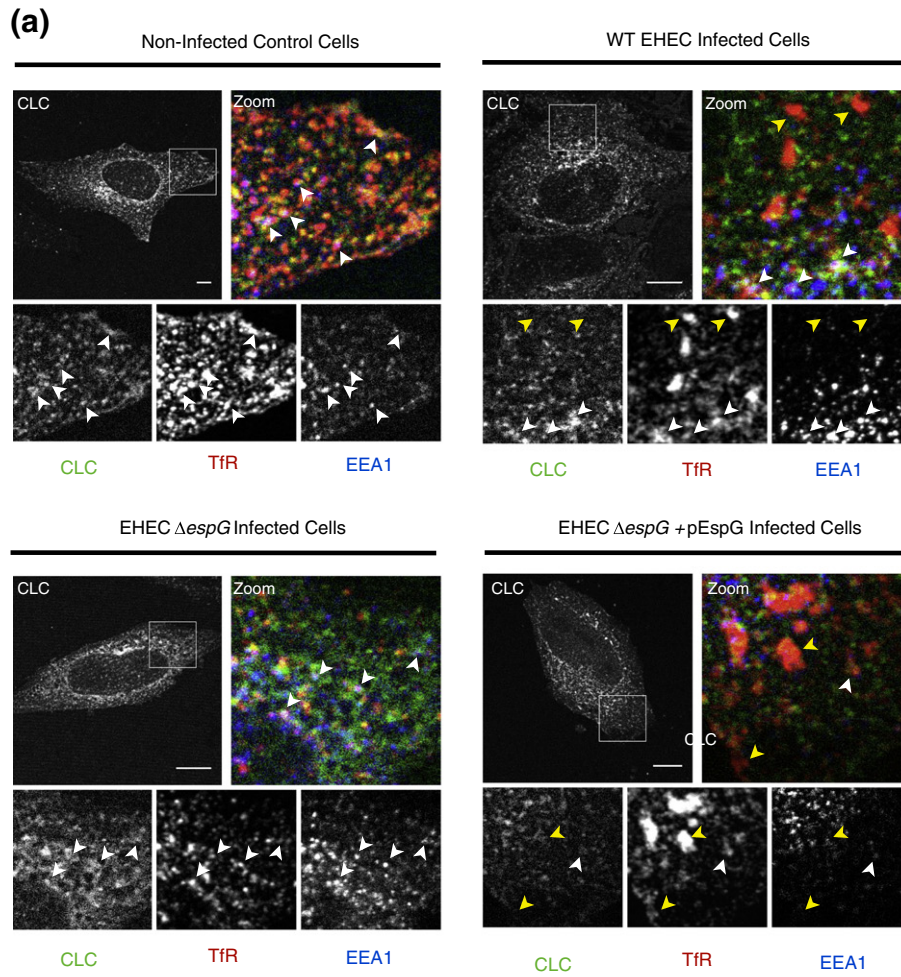


Fig. 4 (legend on next page)

appears to have no effect on CCV uncoating, whilst large TfR positive but EEA1 and Clathrin negative structures occur in the presence of EspG. We therefore hypothesize that EspG potentiates its effects via the modulation of Rab35 specifically on recycling endosomes. Inactivation of Rab35 involved in recycling would give rise to the reduced cell surface proteins we [4], and others [8,10] have previously observed during EHEC/EPEC infection. Consistent with this hypothesis, it was recently reported that knock-down of Rab35 in T_H2 cells interferes with TfR recycling [36]. The RE vesiculation regulators EHD1 and GRAF1 form a complex with MICAL-L1 to promote budding of REs back to the PM [31,35]. As MICAL-L1 can be recruited to REs by Rab35 [32], the inactivation of Rab35 by EspG may prevent RE vesiculation. This closely matches the phenotype observed when Rab35 function is perturbed by other means [37], but further work is required to fully uncover the details of EspGs effect on RE vesiculation.

Whilst a number of reports in the literature have identified ARF6 and Rab35 individually as targets during bacterial infection (ARF6 is implicated in host cell invasion by both *Shigella flexneri* [38] and *Salmonella enterica* serovar Typhimurium [39] and Rab35 is known to be modulated by both uropathogenic *E. coli* (UPEC) [40] and the *Legionella pneumophila* Dot/Icm effector AnkX [41]) concurrent modulation of the ARF6:Rab35 signaling axis by EHEC EspG represents a previously unappreciated strategy of host cell modulation by a bacterial pathogen. As such, this work not only increases our understanding of the plethora of mechanisms bacterial pathogens use to subvert host cell functions but will also contribute to our understanding of the wide variety of fundamental host cell processes that ARF6 and Rab35 have been implicated in, including the AKT signaling pathway [42], sorting of newly endocytosed cargo from the plasma membrane [43], cytokinesis [44] and the establishment of epithelial cell polarity [45].

Acknowledgements

We would like to thank Feng Shao, Philippe Chavrier and Mitsunori Fukuda for numerous constructs. This research was supported by grants

from the Medical Research Council and The Royal Society.

Author Contributions: RCF and AC designed the experiments. RCF, SS and AC performed the experiments. RCF and AC wrote the manuscript with input and discussion from all authors. The authors declare no competing financial interests.

Appendix A. Supplementary data

Supplementary data to this article can be found online at <http://dx.doi.org/10.1016/j.jmb.2016.05.023>.

Received 1 February 2016;

Received in revised form 19 May 2016;

Accepted 20 May 2016

Available online 31 May 2016

Keywords:

Type 3 secretion system, EspG; host-pathogen interactions; small GTPase signaling; endosomal recycling; cargo trafficking

Abbreviations used:

ARF, ADP ribosylation factor; T3SS, Type III secretion system; PM, plasma membrane; RE, recycling endosome; TfR, transferrin receptor; GFP, green fluorescent protein; A/E, attaching and effacing; *E. coli*, *Escherichia coli*; OCRL, oculocerebrorenal syndrome of Lowe; CCV, clathrin coated vesicles; EEA1, early endosome antigen 1; CLC, clathrin light chain.

References

- [1] A.R. Wong, J.S. Pearson, M.D. Bright, D. Munera, K.S. Robinson, S.F. Lee, G. Frankel, E.L. Hartland, Enteropathogenic and enterohaemorrhagic *Escherichia coli*: even more subversive elements, *Mol Microbiol* 80 (2011) 1420–1438.
- [2] R.M. Lynn, S.J. O'Brien, C.M. Taylor, G.K. Adak, H. Chart, T. Cheasty, J.E. Coia, I.A. Gillespie, M.E. Locking, W.J. Reilly, H.R. Smith, A. Waters, G.A. Willshaw, Childhood hemolytic uremic syndrome, United Kingdom and Ireland, *Emerg Infect Dis* 11 (2005) 590–596.

Fig. 4. EspG has no effect on the uncoating of TfR/EEA1 positive vesicles a) HeLa cells expressing mRFP-CLC were infected with EHEC WT, a $\Delta espG$ mutant or $\Delta espG$ + pEspG:4xHA. After 5 h of infection cells were fixed and labeled for EEA1 and TfR. During WT EHEC infection, enlarged TfR positive, EEA1/CLC negative structures can be seen in infected cells. These structures were not observed in non-infected cells, nor those infected with EHEC $\Delta espG$, but were more pronounced in cells infected with EHEC $\Delta espG$ + pEspG:4xHA. Scale bars represent 10 μ m, white arrow heads indicate triple-positive structures, yellow arrow heads indicate large TfR-positive structures lacking EEA1/CLC. b) Quantification of images shows that EspG has no effect on the association of clathrin with TfR positive early endosomes ($n = 2$, > 150 EEA1/TfR positive structures scored per condition per experiment, graph is representative of one independent experiment, ns = non-significant).

- [3] H. Trachtman, HUS and TTP in Children, *Pediatr Clin North Am* 60 (2013) 1513–1526.
- [4] A. Clements, C.A. Stoneham, R.C. Furniss, G. Frankel, Enterohaemorrhagic *Escherichia coli* inhibits recycling endosome function and trafficking of surface receptors, *Cell Microbiol* 16 (2014) 1693–1705.
- [5] E.M. van Dam, T. Ten Broeke, K. Jansen, P. Spijkers, W. Stoorvogel, Endocytosed transferrin receptors recycle via distinct dynamin and phosphatidylinositol 3-kinase-dependent pathways, *J Biol Chem* 277 (2002) 48876–48883.
- [6] Z. Szatmari, V. Kis, M. Lippai, K. Hegedus, T. Farago, P. Lorincz, T. Tanaka, G. Juhasz, M. Sass, Rab11 facilitates cross-talk between autophagy and endosomal pathway through regulation of Hook localization, *Mol Biol Cell* 25 (2014) 522–531.
- [7] C. Hu, D. Hardee, F. Minnear, Membrane fusion by VAMP3 and plasma membrane t-SNAREs, *Exp Cell Res* 313 (2007) 3198–3209.
- [8] L.G. Glotfelty, A. Zahs, K. Hodges, K. Shan, N.M. Alto, G.A. Hecht, Enteropathogenic *E. coli* effectors EspG1/G2 disrupt microtubules, contribute to tight junction perturbation and inhibit restoration, *Cell Microbiol* 16 (2014) 1767–1783.
- [9] R.K. Gill, A. Borthakur, K. Hodges, J.R. Turner, D.R. Clayburgh, S. Saksena, A. Zaheer, K. Ramaswamy, G. Hecht, P.K. Dudeja, Mechanism underlying inhibition of intestinal apical Cl/OH exchange following infection with enteropathogenic *E. coli*, *J Clin Invest* 117 (2007) 428–437.
- [10] T. Gujral, A. Kumar, S. Priyamvada, S. Saksena, R.K. Gill, K. Hodges, W.A. Alrefai, G.A. Hecht, P.K. Dudeja, Mechanisms of DRA recycling in intestinal epithelial cells: effect of enteropathogenic *E. coli*, *Am J Physiol Cell Physiol* 309 (2015) C835–C846.
- [11] S.J. Elliott, E.O. Krejany, J.L. Mellies, R.M. Robins-Browne, C. Sasakawa, J.B. Kaper, EspG, a novel type III system-secreted protein from enteropathogenic *Escherichia coli* with similarities to VirA of *Shigella flexneri*, *Infect Immun* 69 (2001) 4027–4033.
- [12] F.L. Tomson, V.K. Viswanathan, K.J. Kanack, R.P. Kanteti, K.V. Straub, M. Menet, J.B. Kaper, G. Hecht, Enteropathogenic *Escherichia coli* EspG disrupts microtubules and in conjunction with Orf3 enhances perturbation of the tight junction barrier, *Mol Microbiol* 56 (2005) 447–464.
- [13] T. Matsuzawa, A. Kuwae, A. Abe, Enteropathogenic *Escherichia coli* type III effectors EspG and EspG2 alter epithelial paracellular permeability, *Infect Immun* 73 (2005) 6283–6289.
- [14] R.K. Shaw, K. Smollett, J. Cleary, J. Garmendia, A. Straatman-Iwanowska, G. Frankel, S. Knutton, Enteropathogenic *Escherichia coli* type III effectors EspG and EspG2 disrupt the microtubule network of intestinal epithelial cells, *Infect Immun* 73 (2005) 4385–4390.
- [15] P.R. Hardwidge, W. Deng, B.A. Vallance, I. Rodriguez-Escudero, V.J. Cid, M. Molina, B.B. Finlay, Modulation of host cytoskeleton function by the enteropathogenic *Escherichia coli* and *Citrobacter rodentium* effector protein EspG, *Infect Immun* 73 (2005) 2586–2594.
- [16] K.L. Germane, R. Ohi, M.B. Goldberg, B.W. Spiller, Structural and functional studies indicate that *Shigella* VirA is not a protease and does not directly destabilize microtubules, *Biochemistry* 47 (2008) 10241–10243.
- [17] P. Dean, S. Muhlen, S. Quitard, B. Kenny, The bacterial effectors EspG and EspG2 induce a destructive calpain activity that is kept in check by the co-delivered Tir effector, *Cell Microbiol* 12 (2010) 1308–1321.
- [18] A. Clements, K. Smollett, S.F. Lee, E.L. Hartland, M. Lowe, G. Frankel, EspG of enteropathogenic and enterohemorrhagic *E. coli* binds the Golgi matrix protein GM130 and disrupts the Golgi structure and function, *Cell Microbiol* 13 (2011) 1429–1439.
- [19] K.L. Germane, B.W. Spiller, Structural and functional studies indicate that the EPEC effector, EspG, directly binds p21-activated kinase, *Biochemistry* 50 (2011) 917–919.
- [20] A.S. Selyunin, S.E. Sutton, B.A. Weigele, L.E. Reddick, R.C. Orchard, S.M. Bresson, D.R. Tomchick, N.M. Alto, The assembly of a GTPase-kinase signalling complex by a bacterial catalytic scaffold, *Nature* 469 (2011) 107–111.
- [21] N. Dong, Y. Zhu, Q. Lu, L. Hu, Y. Zheng, F. Shao, Structurally distinct bacterial TBC-like GAPs link Arf GTPase to Rab1 inactivation to counteract host defenses, *Cell* 150 (2012) 1029–1041.
- [22] L.A. Volpicelli-Daley, Y. Li, C.J. Zhang, R.A. Kahn, Isoform-selective effects of the depletion of ADP-ribosylation factors 1–5 on membrane traffic, *Mol Biol Cell* 16 (2005) 4495–4508.
- [23] E. Macia, F. Luton, M. Partisani, J. Cherfils, P. Chardin, M. Franco, The GDP-bound form of Arf6 is located at the plasma membrane, *J Cell Sci* 117 (2004) 2389–2398.
- [24] G. Montagnac, H. de Forges, E. Smythe, C. Gueudry, M. Romao, J. Salamero, P. Chavrier, Decoupling of activation and effector binding underlies ARF6 priming of fast endocytic recycling, *Curr Biol* 21 (2011) 574–579.
- [25] A.S. Selyunin, L.E. Reddick, B.A. Weigele, N.M. Alto, Selective Protection of an ARF1-GTP Signaling Axis by a Bacterial Scaffold Induces Bidirectional Trafficking Arrest, *Cell Rep* 6 (2014) 878–891.
- [26] A.H. Hutagalung, P.J. Novick, Role of Rab GTPases in membrane traffic and cell physiology, *Physiol Rev* 91 (2011) 119–149.
- [27] H. Stenmark, Rab GTPases as coordinators of vesicle traffic, *Nat Rev Mol Cell Biol* 10 (2009) 513–525.
- [28] J.B. Pereira-Leal, M.C. Seabra, Evolution of the Rab family of small GTP-binding proteins, *J Mol Biol* 313 (2001) 889–901.
- [29] C. Cauvin, M. Rosendale, N. Gupta-Rossi, M. Rocancourt, P. Larraufie, R. Salomon, D. Perrais, A. Echard, Rab35 GTPase Triggers Switch-like Recruitment of the Lowe Syndrome Lipid Phosphatase OCRL on Newborn Endosomes, *Curr Biol* 26 (2016) 120–128.
- [30] P.D. Allaire, M. Seyed Sadr, M. Chaineau, E. Seyed Sadr, S. Konefal, M. Fotouhi, D. Maret, B. Ritter, R.F. Del Maestro, P.S. McPherson, Interplay between Rab35 and Arf6 controls cargo recycling to coordinate cell adhesion and migration, *J Cell Sci* 126 (2013) 722–731.
- [31] H. Kobayashi, M. Fukuda, Rab35 establishes the EHD1-association site by coordinating two distinct effectors during neurite outgrowth, *J Cell Sci* 126 (2013) 2424–2435.
- [32] H. Kobayashi, K. Etoh, N. Ohbayashi, M. Fukuda, Rab35 promotes the recruitment of Rab8, Rab13 and Rab36 to recycling endosomes through MICAL-L1 during neurite outgrowth, *Biol Open* 3 (2014) 803–814.
- [33] A.L. Marat, P.S. McPherson, The connecdenn family, Rab35 guanine nucleotide exchange factors interfacing with the clathrin machinery, *J Biol Chem* 285 (2010) 10627–10637.
- [34] S. Xie, N. Naslavsky, S. Caplan, Diacylglycerol kinase alpha regulates tubular recycling endosome biogenesis and major histocompatibility complex class I recycling, *J Biol Chem* 289 (2014) 31914–31926.
- [35] B. Cai, S. Xie, S. Caplan, N. Naslavsky, GRAF1 forms a complex with MICAL-L1 and EHD1 to cooperate in tubular

- recycling endosome vesiculation, *Front Cell Dev Biol* 2 (2014) 22.
- [36] C.W. Yang, C.D. Hojer, M. Zhou, X. Wu, A. Wuster, W.P. Lee, B.L. Yaspan, A.C. Chan, Regulation of T Cell Receptor Signaling by DENND1B in TH2 Cells and Allergic Disease, *Cell* 164 (2016) 141–155.
- [37] P.D. Allaire, A.L. Marat, C. Dall'Armi, G. Di Paolo, P.S. McPherson, B. Ritter, The Connecdenn DENN domain: a GEF for Rab35 mediating cargo-specific exit from early endosomes, *Mol Cell* 37 (2010) 370–382.
- [38] A.C. Garza-Mayers, K.A. Miller, B.C. Russo, D.V. Nagda, M.B. Goldberg, *Shigella flexneri* Regulation of ARF6 Activation during Bacterial Entry via an IpgD-Mediated Positive Feedback Loop, *MBio* 6 (2015), e02584, <http://dx.doi.org/10.1128/mBio.02584-14>.
- [39] A.C. Davidson, D. Humphreys, A.B. Brooks, P.J. Hume, V. Koronakis, The Arf GTPase-activating protein family is exploited by *Salmonella enterica* serovar Typhimurium to invade nonphagocytic host cells, *MBio* 6 (2015), e02253–14, <http://dx.doi.org/10.1128/mBio.02253-14>.
- [40] N. Dikshit, P. Bist, S.N. Fenlon, N.K. Pulloor, C.E. Chua, M.A. Scidmore, J.A. Carlyon, B.L. Tang, S.L. Chen, B. Sukumaran, Intracellular Uropathogenic *E. coli* Exploits Host Rab35 for Iron Acquisition and Survival within Urinary Bladder Cells, *PLoS Pathog* 11 (2015), e1005083, <http://dx.doi.org/10.1371/journal.ppat.1005083>.
- [41] S. Mukherjee, X. Liu, K. Arasaki, J. McDonough, J.E. Galan, C.R. Roy, Modulation of Rab GTPase function by a protein phosphocholine transferase, *Nature* 477 (2011) 103–106.
- [42] D.B. Wheeler, R. Zoncu, D.E. Root, D.M. Sabatini, C.L. Sawyers, Identification of an oncogenic RAB protein, *Science* 350 (2015) 211–217.
- [43] D. Dutta, J.G. Donaldson, Sorting of Clathrin-Independent Cargo Proteins Depends on Rab35 Delivered by Clathrin-Mediated Endocytosis, *Traffic* 16 (2015) 994–1009.
- [44] L. Chesneau, D. Dambournet, M. Machicoane, I. Kouranti, M. Fukuda, B. Goud, A. Echard, An ARF6/Rab35 GTPase cascade for endocytic recycling and successful cytokinesis, *Curr Biol* 22 (2012) 147–153.
- [45] K. Klinkert, M. Rocancourt, A. Houdusse, A. Echard, Rab35 GTPase couples cell division with initiation of epithelial apico-basal polarity and lumen opening, *Nat Commun* 7 (2016), 11166, <http://dx.doi.org/10.1038/ncomms11166>.